Structural Engineering and Mechanics, *Vol. 62, No. 6 (2017) 739-748*
DOI: https://doi.org/10.12989/sem.2017.62.6.739

Influence of laser peening on fatigue crack initiation of notched aluminum plates

Vignaud Granados-Alejo[1b], Carlos Rubio-Gonzalez[*1], Yazmin Parra-Torres[1b], J. Antonio Banderas[1b] and Gilberto Gómez-Rosas[2a]

[1]*Centro de Ingeniería y Desarrollo Industrial, Pie de la Cuesta. 702, Desarrollo San Pablo, Querétaro, Qro.,76125, México*
[2]*Universidad de Guadalajara, Guadalajara, Jal. México*

(Received January 21, 2017, Revised April 11, 2017, Accepted April 12, 2017)

Abstract. Notches such as slots are typical geometric features on mechanical components that promote fatigue crack initiation. Unlike for components with open hole type notches, there are no conventional treatments to enhance fatigue behavior of components with slots. In this work we evaluate the viability of applying laser shock peening (LSP) to extend the fatigue life of 6061-T6 aluminum components with slots. The feasibility of using LSP is evaluated not only on damage free notched specimens, but also on samples with previous fatigue damage. For the LSP treatment a convergent lens was used to deliver 0.85 J and 6 ns laser pulses 1.5 mm in diameter by a Q-switch Nd: YAG laser, operating at 10 Hz with 1064 nm of wavelength. Residual stress distribution was assessed by the hole drilling method. A fatigue analysis of the notched specimens was conducted using the commercial code FE-Safe and different multiaxial fatigue criteria to predict fatigue lives of samples with and without LSP. The residual stress field produced by the LSP process was estimated by a finite element simulation of the process. A good comparison of the predicted and experimental fatigue lives was observed. The beneficial effect of LSP in extending fatigue life of notched components with and without previous damage is demonstrated.

Keywords: laser shock processing; fatigue damage; fatigue life; residual stress

1. Introduction

Laser Shock Peening (LSP) is a surface treatment technique that has been shown to be effective in improving the fatigue properties of a number of metals and alloys. Potential applications are directed to aerospace and automotive industries. Peyre and Fabro (1995) provides deep revision of LSP trends related to the physics, the mechanics and the applications involved. Static, cyclic, fretting fatigue and stress corrosion performance are some properties that have been improved by LSP for different materials. For aluminum alloys, Yang *et al*. (2001) demonstrated the effectiveness of LSP on the fatigue behavior of specimens with a fastener hole, multiple crack stopholes and single-edge notch. The fatigue behavior improvements on samples were attributed to a combination of increased dislocation density and compressive residual stress induced by the laser shock waves according to results reported by Hong and Chengye (1998). Rubio-Gonzalez *et al*. (2004) demonstrated that LSP reduces fatigue crack growth and increases fracture toughness in an aluminum alloy and in a duplex stainless steel (Rubio-Gonzalez *et al*. 2011) while wear rate decreases by using LSP as shown by Sanchez-Santana *et al*. (2011). The effect of an absorbent overlay on the residual stress field induced by LSP was analyzed by Rubio-Gonzalez *et al*. (2006), it was observed that the overlay makes the compressive residual stress profile move to the surface. On the other hand, for steels and nickel-based alloys, beneficial effects provided by LSP have been reported. Tsay *et al*. (2003) evaluated the fatigue crack growth behavior of laser-processed 304 stainless steel in air and gaseous hydrogen; on both cases, a lower fatigue crack growth was observed. Lavender *et al*. (2008) used the LSP process to increase life of pilger dies made of A2 tool steel by imparting compressive residual stresses to failure prone areas of the dies. The fatigue behavior improvement of LSP treated aluminum friction stir welded joints has been also evaluated by Hatamleh *et al*. (2007) and Hatamleh (2009), the results indicate a significant reduction in fatigue crack growth rates using LSP compared to SP and native welded specimens. However, at cryogenic temperature, it was difficult to discern a trend between residual stress treatment and crack growth rate data as demonstrated by Hatamleh *et al*. (2009); laser peening over the friction stir welded material resulted in the fatigue crack growth rates being comparable to those for base material.

Some works have been reported the LSP effect on plates with holes. The effect of residual stress on fatigue behavior and crack propagation from LSP-worked hole was investigated by Ren *et al*. (2013). The degree to which the fatigue response of geometric features can be modelled by using eigenstrain distributions was investigated experimentally and numerically by Achintha *et al*. (2014). The effects of various laser shock peening patterns on the residual stress distribution and fatigue performance of Ti–

∗Corresponding Author, Ph.D.
E-mail: crubio@cidesi.edu.mx
[a]Ph.D.
[b]Ph.D. Student

ISSN: 1225-4568 (Print), 1598-6217 (Online)

6Al-4V open hole fatigue samples has been investigated by Cuellar *et al*. (2012). The contour method was used to determine the residual stress induced by LSP. A correlation between the residual stress distribution and fatigue performance was established. Ivetic *et al*. (2012) evaluated the effect of the sequence of operations on the effectiveness of LSP treatment in improving the fatigue performance of open hole aluminum specimens.

Numerical simulations of the LSP have been demonstrated to be useful in order to evaluate the effect of changing process parameters and analyze the response on different materials. Ocaña *et al*. (2004) developed a FE model to estimate residual stresses and surface deformation induced by LSP using different process parameters. Ivetic (2011) used a 3D FE analysis to determine the response of aluminum alloy thin plates including the effect of wave reflections from the plate back side. A FE simulation of multiple LSP impacts was presented by Ding and Ye (2006) to estimate the magnitude and distribution of residual stresses on steel samples. A numerical analysis of an open hole specimen subjected to LSP was conducted by Ivetic *et al*. (2011), the effect of the induced residual stress field on the fatigue life of the specimen was investigated. A fully 3D finite element model was used by Correa *et al*. (2015) to predict the residual stresses and optimize the LSP in order to increase the fatigue life of materials.

It is known that the residual stress field due to LSP is extremely sensitive to geometric features (Cuellar *et al*. 2012) and it is well understood that geometric details, such as notches or holes, are typical fatigue crack initiation points because they act as stress concentrators. The effect of LSP on fatigue properties of a notched 7075-T6 aluminum plate has been investigated by Zhang *et al*. (2015), it was demonstrated that the location of fatigue crack initiation was transferred from top surface to sub-surface.

Several mechanical components of practical interest have slots and notches can not be avoided. These geometric details are stress concentrators that reduce load capacity and are prone places for fatigue crack initiation. Compressive residual stresses are beneficial as they tend to cancel with the stress resulting from external loading thus reducing the effective stress concentration at the slot tip and the likelihood of fatigue crack initiating under fluctuating loading is reduced. While there are some techniques to improve fatigue life of components containing holes, such as cold expansion which generates a compressive residual stress around the hole edge (Chakherlou and Vogwell 2003, Amrouch *et al*. 2003, Larac *et al*. 2000, Liu *et al*. 2008, Rubio-Gonzalez *et al*. 2015); it may be difficult to treat specimens with slots in order to delay fatigue crack initiation around the slot tip. It would be desirable to develop techniques to enhance fatigue life of components with slots or to extend fatigue lives once the components have previous damage.

Only few references are available in the open literature where the effect of LSP on delay crack formation from notches has been analyzed. In addition, no previous work has been reported evaluating the effect of LSP on the behavior of specimens with previous fatigue damage.

The aim of this paper is to investigate the effect of LSP on the fatigue behavior of notched 6061-T6 aluminum alloy plates with and without previous fatigue damage. The beneficial effect of LSP in extending the fatigue life of previously damaged notched components is demonstrated. A finite element simulation of the LSP process on notched samples followed by a fatigue analysis employing multiaxial fatigue criteria to predict fatigue life is also presented. Predicted lives are compared with experimental results in order to assess different fatigue criteria. The LSP simulation was performed using the commercial code ABAQUS and the fatigue analysis was made employing the code FE-Safe using as input the residual stresses obtained in the previous LSP simulation.

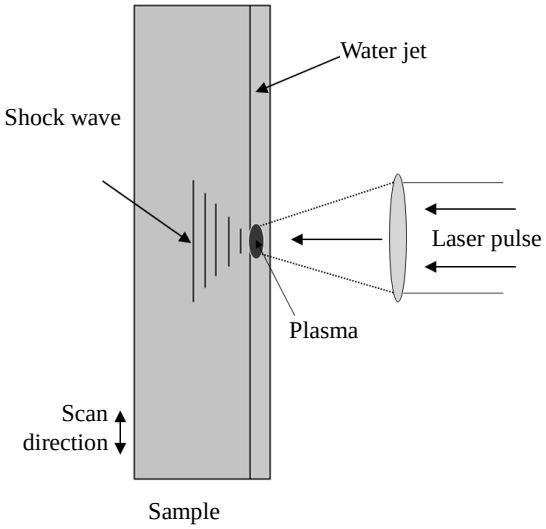

Fig. 1 Principle of Laser Shock Processing

In the laser shock processing of metals, the sample is either completely immersed in water or in air. A water jet may be used also to produce a water wall with constant thickness on the sample. The laser pulse is then focused onto the sample. The schematic of how the process works in water is shown in Fig. 1. When the laser beam is directed onto the surface to be treated, it passes through the transparent overlay and strikes the sample. It immediately vaporizes a thin surface layer of the overlay. High pressure against the surface of the sample causes a shock wave to propagate into the material. The plastic deformation caused by the shock wave produces the compressive residual stresses at the surface of the sample.

2. Experimental procedure

Material

Specimens were obtained from plates of 6061-T6 aluminum alloy with thickness of 12.9 mm. The T6 condition consists of a solution treatment and artificial aging. The thickness of all specimens was reduced from 12.9 mm to 5 mm by machining the specimen faces to eliminate the manufacturing effect of the original plates. Chemical composition was: 0.66 wt % Si, 0.22 wt % Fe,

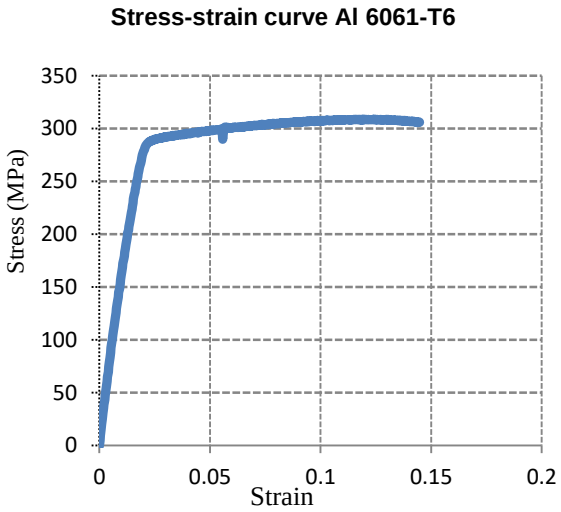

Fig. 2 Stress-strain curve of 6061-T6 aluminum alloy under tensile loading conditions

0.26 wt % Cu, 0.03 wt % Mn, 0.85 wt % Mg, 0.02 wt % Zn, 0.01 wt % Ni, 0.045 wt % Cr, 0.013 wt % Ti. The chemical composition was determined using a spark emission spectrometer. The mechanical properties were determined using dog-bone type specimens with strain rate of 1 mm/min. Results are shown in Fig. 2. The offset tensile yield stress is 288.5 MPa, ultimate tensile strength 309.1 MPa and elastic modulus 63.2 GPa. The specimens used for residual stress measurement were blocks of 50×50×5 mm with LSP on both sides. The specimen used for fatigue crack initiation and growth tests were compact tension type specimens as illustrated in Fig. 3. All fatigue crack growth tests specimens were machined with the loading axis parallel to the rolling direction. Fig. 3(a) also illustrates pulse swept direction.

Laser shock processing

The LSP experiments were performed using a Q switched Nd:YAG laser operating at 10 Hz with a wave length of 1064 nm, the FWHM of the pulses was 6 ns. A convergent lens was used to deliver 0.85 J/pulse. Spot diameter was 1.5 mm. Pulse density was 2500 pul/cm^2. A special device to produce a controlled water jet was implemented to form a thin water layer on the sample to be treated. Specimen treated area was 25×25 mm on both sides of the compact tension specimen. A 2D motion system was used to control specimen position and generate the pulse swept as shown in Fig. 3. Controlling the velocity of the system, the desired pulse density was obtained. No protective coating was used during LSP (Rubio-Gonzalez *et al*. 2006). Fig. 3(b) shows a photograph of a compact tension specimen with LSP.

Fatigue crack initiation and growth

Fatigue crack initiation and growth tests were performed on a MTS 810 servo-hydraulic system at room temperature in the air. Load ratio $R=P_{min}/P_{max}$ was maintained at R=0.1. Frequency of 15 Hz with a sine wave form was used in the experiments. Each specimen was tested to maximum load of 3 kN. Fatigue crack initiation life was considered when a small crack of about 2 mm long appeared on the surface.

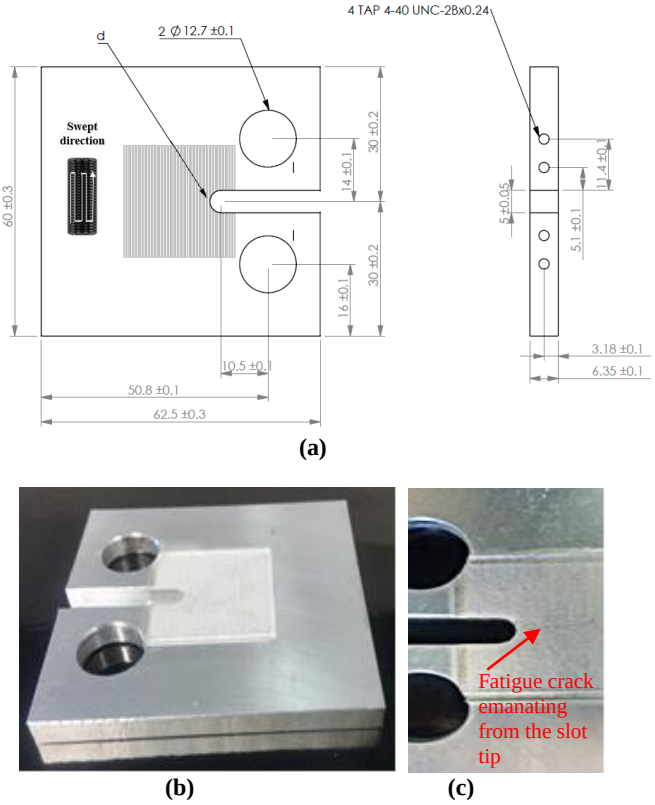

Fig. 3 Compact tension test type specimens used in the fatigue crack initiation and growth tests. (a) Specimen geometry, dimensions in mm (b) Specimen with LSP (c) Initiation crack on tested specimen

Two slot tip diameters (and therefore slot width) were considered, d=3 mm and d=5 mm.

Fatigue damage accumulation may be defined by the simple rule $D=n/N_f$ where n and N_f are the applied cycles and applied cycles to failure under constant amplitude load level, respectively. Fatigue life recorded under this loading condition was N_f=37,466 for specimens with slot width d=3 mm and N_f=222,542 for samples with slot width d=5 mm.

Once fatigue life was known, fatigue damage was induced on notched specimens at damage levels of D=0.25 and 0.5. For example, specimens with d=5 mm were subjected to 55,636 cycles of loading to generate a fatigue damage D=0.25. LSP was applied on specimens with and without previous fatigue damage.

Residual stress measurement

The residual stress was measured using the hole drilling method as specified by the ASTM 837 standard. In this work a hole of 1.6 mm in diameter at a depth approximately of 1 mm was made on the specimen surface. A three element rosette measured the strain relief in the material around the hole. Residual stresses existing in the material before hole drilling can be determined from the measured relieved strains. Strain gage rosettes CEA-06-062UL-120 along with a RS-200 Milling Guide from Measurements Group were used.

3. Modelling

Finite Element Analysis

A simplified FEM simulation of the LSP process was performed using the commercial code ABAQUS/Explicit. The purpose of this analysis was to obtain a qualitative residual stress distribution that then may be used in a fatigue analysis.

The approach used for the FEM modelling was to analyze the transient response of the treated sample due to the pressure of the created plasma, rather than modelling the real LSP process itself. A similar approach has been used by Ivetic *et al*. (2012). Two steps constitute the numerical analysis; a loading step in which the laser pulse is applied followed by a relaxation step where the model returns to the equilibrium state. The model is shown in Fig. 4 in which 48,180 C3D8R linear hexahedron elements were used. The mesh around the slot tip was denser with respect to the rest of the model. The mesh density is within the parameters studied by Ding (2003). Encastre boundary condition was applied on the specimen back face edge while LSP was applied on the front face simulating the fixed condition used during the LSP treatment. After this step, the process was inverted in order to treat both specimen faces.

The simulated loading condition was a pressure pulse on 25 mm×25 mm square, with time evolution in nanoseconds (ns) given in Table 1. Peak pressure of 5.21 GPa was obtained according with Hfaideh *et al*. (2015). These process conditions were chosen to simplify the real process where a full analysis would consider high density of smaller laser peens. That is, the simplified analysis simulated only one big laser peen.

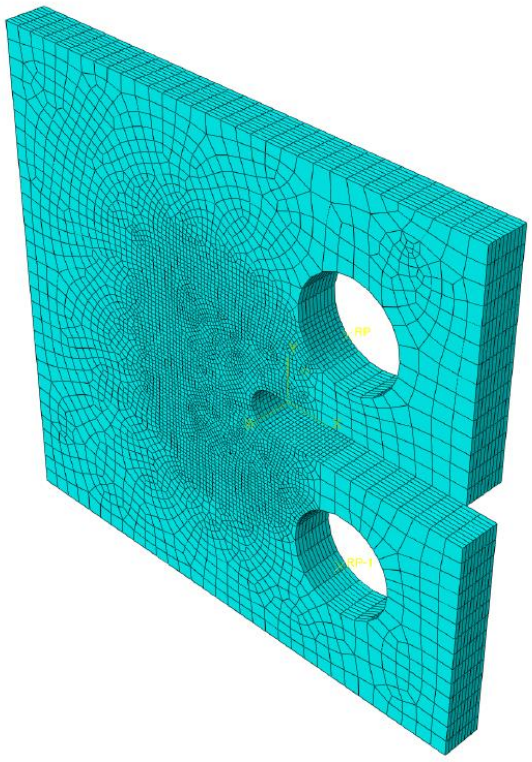

Fig. 4 Finite element model of the specimen

The material model used to simulate the behavior of the material under the shock conditions was the Johnson-Cook model

$$\sigma = \left(A + B\varepsilon_{eq}^{n}\right)\left[1 + C\,\mathrm{In}\left(\frac{\dot{\varepsilon}}{\dot{\varepsilon}_0}\right)\right]\left[1 - \left(\frac{T - T_0}{T_m - T_0}\right)^{m}\right] \quad (1)$$

with material constants given in Table 2 (Ivetic *et al*. 2012, Goel 2015).

Multiaxial fatigue criteria

Fatigue lives under constant amplitude loading were correlated by the Coffin–Manson equation:

$$\frac{\Delta_\varepsilon}{2} = \frac{\sigma_f'}{E}\left(2N_f\right)^b + \varepsilon_f'\left(2N_f\right)^c \quad (2)$$

where Δ_ε is the strain range in axial fatigue, N_f is the number of cycles to failure, E is the Young's modulus, σ_f' and ε_f' are the axial fatigue strength coefficient and fatigue ductility coefficient, respectively; b and c are the axial fatigue strength exponent and fatigue ductility exponent, respectively. This equation is used as the basis for establishing the fatigue parameter vs. life relations for multiaxial fatigue.

In the critical plane approaches for multiaxial fatigue analysis, the fatigue life prediction is based on the continuum mechanics variables on the physical crack plane, called critical plane. The Brown-Miller equation, one of the first critical plane theories, proposes that the maximum fatigue damage occurs at the plane which experiences the maximum shear strain amplitude, and that the damage is a function of both this shear strain and the strain normal to this plane. Stress-based Brown-Miller derives from this to give a superior fatigue damage assessment for high cycle fatigue with complex axial and torsional loading, and is suitable for ductile metals (Brown and Miller 1973). Kandil, Brown and Miller produced a variant of the Brown-Miller equation that can be used with conventional uniaxial materials databases (Kandil *et al*. 1982)

$$\frac{\Delta_\gamma}{2} + \frac{\Delta_{\varepsilon_n}}{2} = 1.65\,\frac{\left(\sigma_f' - \sigma_m\right)}{E}\left(2N_f\right)^b + 1.75\varepsilon_f'\left(2N_f\right)^c \quad (3)$$

The Brown-Miller equation gives the most realistic life estimates for ductile metals, and tends to be non-conservative for brittle metals. Brown-Miller and Principal Stress theories for fatigue analysis are considered in this work.

Several relations to estimate Coffin-Manson parameters from monotonic properties have been proposed in the literature (Li *et al*. 2011). Relations used in this work: Uniform material law, Medians Method and Modified Mitchell´s Method, are given in Table 3.

Different equations have been proposed to consider the effect of mean stress on fatigue life predictions (Dowling 2007). In this work the Morrow and SWT (Smith, Watson and Topper) relations were considered.

Table 1 Load distribution

Time (ns)	0	10	20	30	35	40	50	60	70	75
Pressure (GPa)	0	1.04	3.12	4.16	5.21	4.68	4.16	3.12	2.08	0

Table 2 Johnson-Cook parameters for Al 6061-T (Ivetic *et al*. 2012, Goel 2015)

A (MPa)	B (MPa)	C	n	m	$\dot{\varepsilon_0}$
288.562	162.1	0.0125	0.2783	1.34	1

Table 3 Estimation methods for Coffin-Manson parameters

Parameter	Uniform material law (Baumel and Seegeer 1990)	Medians method (Meggiolaro and Castro 2004)	Modified Mitchell's Method (Park and Song 2003)
$\sigma_f^{'}$	$1.67\sigma_b$	$1.9\sigma_b$	$\sigma_b + 355$
$\varepsilon_f^{'}$	0.35	0.28	ε_f
b	-0.095	-0.11	$\frac{1}{6} log\left(\frac{\sigma_b + 355}{0.446\sigma_b}\right)$
c	-0.69	-0.66	-0.664

Fatigue Analysis

The commercial code FE-Safe was used for the specimen fatigue analysis to estimate the number of cycles to failure. Once the transient FEM analysis using ABAQUS was conducted the residual stress field was determined, then a load of 3 kN was applied and the resultant stress field (combination of the residual stress due to LSP and the stress due to the external load) was transferred to FE-Safe for the fatigue analysis (FE-Safe Documents 2002). In other words, fatigue simulation was conducted with loading conditions similar to the fatigue experiments; that is: constant amplitude, R=0.1 and a maximum load P_{max}=3 kN. It is worth noting that a fatigue analysis on specimens without LSP was also conducted; in this case the load of 3 kN was applied to the model shown in Fig. 4 and the resulting stress field was then transferred to FE-Safe for the subsequent analysis.

4. Results and discussion

Residual stresses obtained by LSP simulation are shown in Fig. 5. FEM residual stress profiles as a function of depth are plotted. Y-component residual stress is shown where the y-axis is perpendicular to the specimen slot. Stress profiles correspond to points A, B and C located at the slot tip, 4.5 mm from the slot tip and 15 mm from the slot tip, respectively, as illustrated in Fig. 5(b). Note that the highest compressive stress (about 170 MPa) corresponds to point B, on that point the predicted residual stress is compressive even in the center of the specimen. Point C is closer to the boundary of the treated area and it exhibits a lower compressive residual stress value. Note also that the residual stress profiles are approximately symmetric since both specimen surfaces were LSP treated.

Experimental residual stress distribution as a function of depth is shown in Fig. 6. These results were obtained using the hole drilling method (ASTM E837) on square samples without notch. S_{xx} corresponds to the stress component along the swept direction of the LSP treatment and S_{yy} normal to that direction. The highest compressive residual stress produced by LSP is about 150 MPa corresponding to S_{yy} at a depth 0.7 mm. Residual stress results on a specimen without LSP are included for comparison.

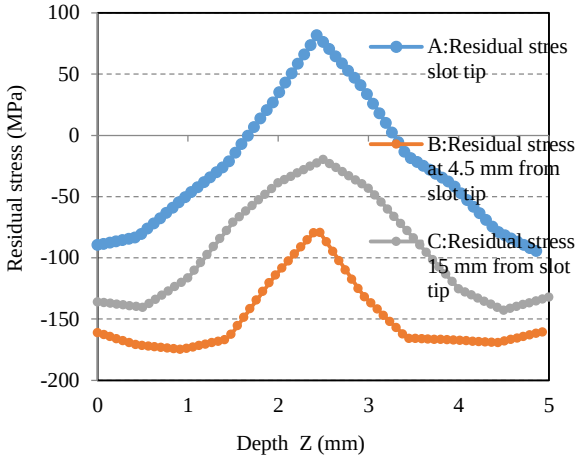

(a)

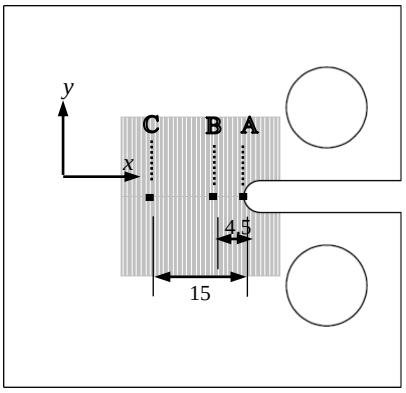

(b)

Fig. 5 (a) Residual stress profiles estimated by simulation, (b) specimen locations where residual stress was determined from LSP simulation, dimensions in mm

Notched samples with previous fatigue damage were then treated with LSP to evaluate its effect in extending fatigue crack initiation life. Results are shown in Fig. 7 where the beneficial effect of LSP can be appreciated. For specimens with slot tip diameter d=5 mm (Fig. 7(a)), fatigue life was extended by 13% on samples with previous damage of D=0.25 and 12% on specimens with D=0.5, considering fatigue life of samples without LSP as a reference. In case of notched specimens with d=3 mm (Fig. 7(b)); LSP extended fatigue life by 43% and 58% on samples with previous damage D=0.25 and D=0.5, respectively, under the same loading conditions. Note that

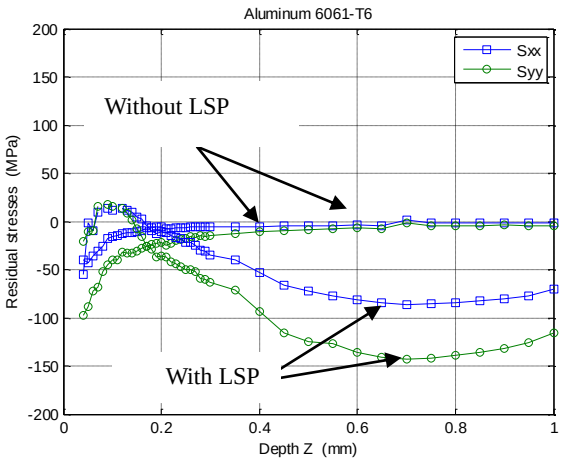

Fig. 6 Experimental residual stresses profiles, with and without LSP

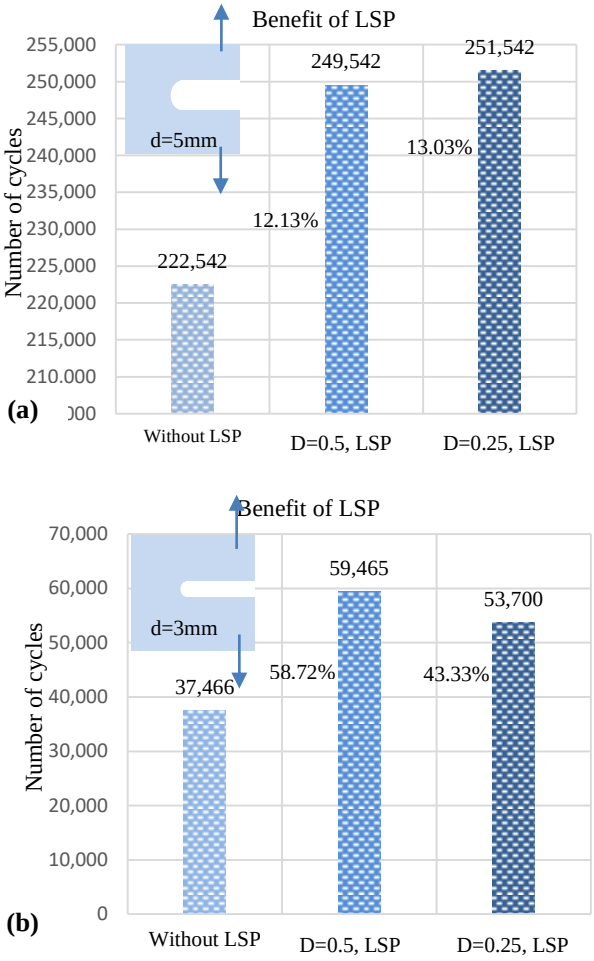

Fig. 7 Improvement on fatigue crack initiation of aluminum samples with different notches and with previous fatigue damage, (a) notch diameter d=5 mm, (b) notch diameter d=3 mm

fatigue life extension is higher in specimens with notch diameter d=3 mm. These results demonstrate the feasibility of using LSP to enhance fatigue properties of components with slots even in the case of sharp slots on specimens with and without previous damage. Residual life of components is prolonged by applying LSP on the surface around the slot tip.

Once the LSP simulation was conducted by using a FEM analysis in ABAQUS, the combined residual stress field and the stress generated by the load of 3 kN is transferred to FE-Safe software for fatigue analysis as illustrated in Fig. 8. Fig. 8(a) shows the residual stress distribution (S_{22} component) on the notched specimen produced by a big laser peen, then a tensile load of 3 kN is applied producing the stress distribution shown in Fig. 8(b) and finally, after the fatigue analysis is performed, a cycles-to-failure distribution is obtained as illustrated in Fig. 8(c). The zoom view of the notch tip in Fig. 8(c) indicates that a lower fatigue life is predicted on the notch tip as it was expected.

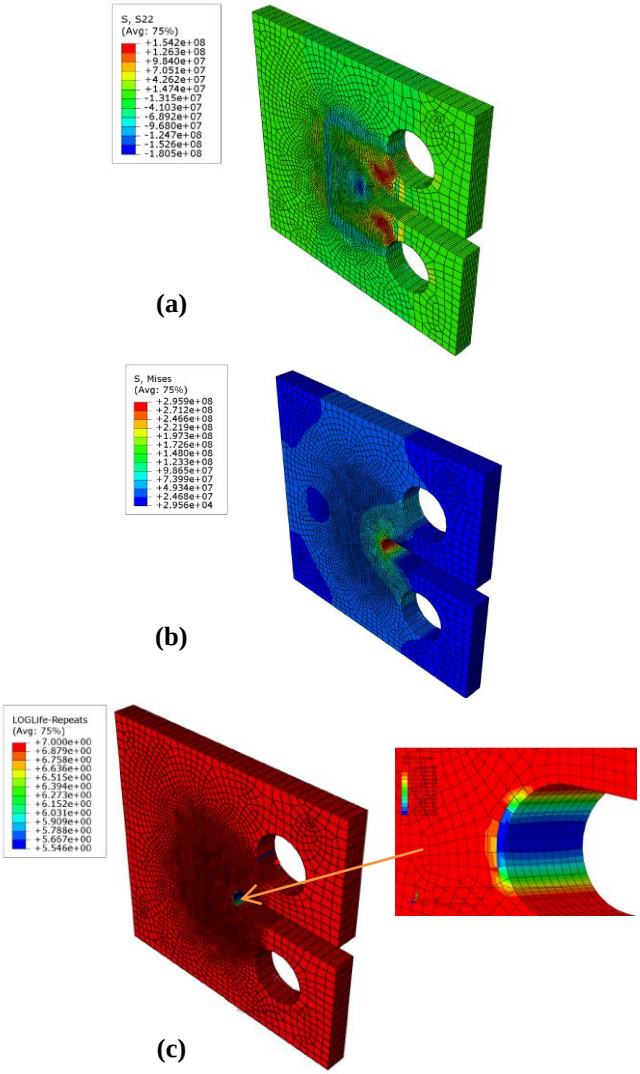

Fig. 8 (a) Residual stress distribution after applying a big laser peen, (b) stress field (von Mises) after applying a 3 kN force, (b) cycles-to-failure distribution obtained by FE-Safe

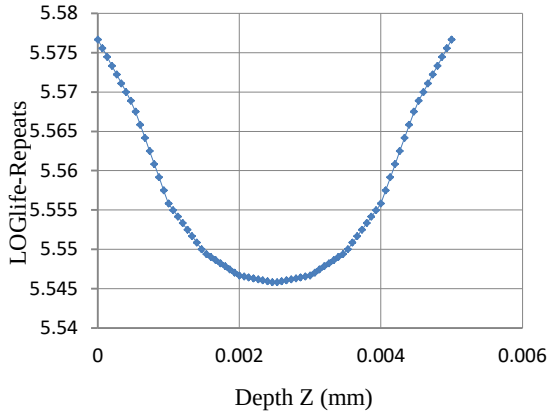

(a)

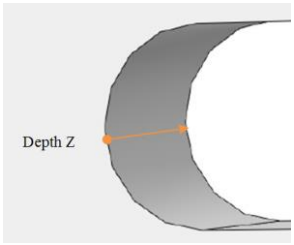

(b)

Fig. 9 (a) Predicted fatigue life on the notch tip as a function of specimen depth, (b) path where predicted fatigue life was evaluated

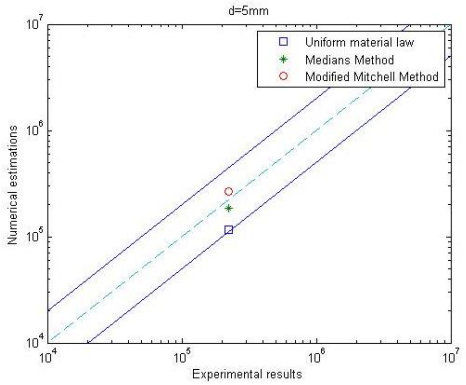

(a)

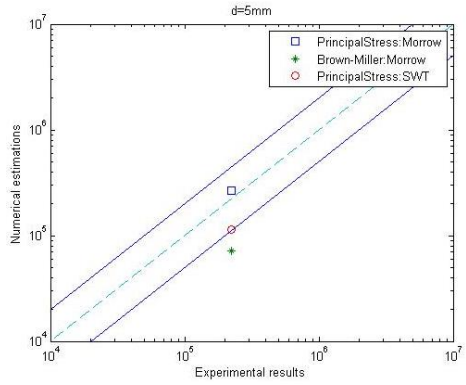

(b)

Fig. 10 (a) Results of variation Coffin-Manson parameters (b) Theories of fatigue multiaxial without residual stress (c) Theories of fatigue multiaxial with residual stress

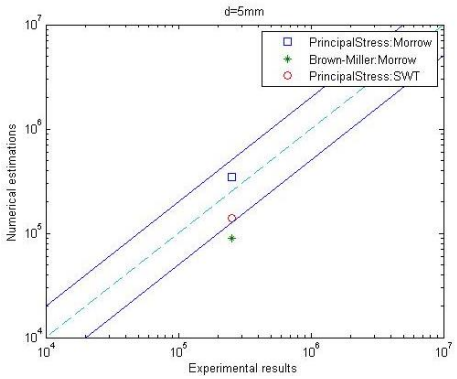

(c)

Fig. 10 Continued

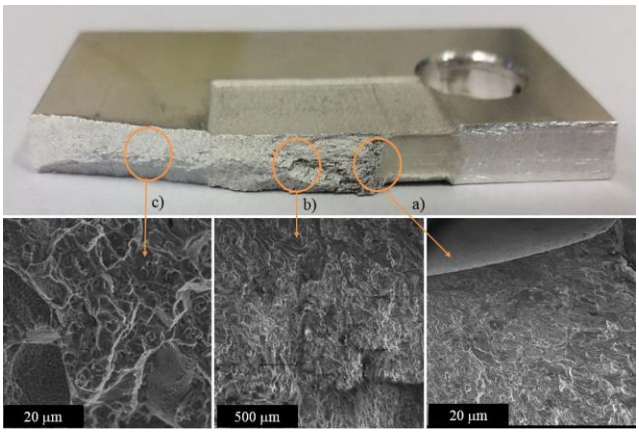

Fig. 11 Fracture surface of a tested specimen with LSP, (a) Crack initiation zone, (b) stable crack growth zone, (c) Final rupture surface

A deeper analysis of estimated fatigue life is given in Fig. 9 where a fatigue life profile as a function of specimen depth is plotted. The path where fatigue life was estimated is also indicated. This result corresponds to a sample with LSP and d=5 mm using the Principal Stress criterion. Note that the fatigue analysis predicts a shorter life on the center of the specimen, about $10^{5.545}$ cycles. This result is in agreement with the residual stress profile "A" of Fig. 5(a) which indicates lower compressive residual stress at the middle of the specimen, in fact, tensile residual stress is predicted and therefore less fatigue life.

A comparison of experimental and predicted fatigue lives is presented in Fig. 10 where the usual factor-2 scatter bands are plotted as well. Fig. 10(a) illustrates the results obtained by using the Principal Stress criterion for fatigue analysis and three different models to estimate parameters of the Coffin-Manson equation mentioned in Table 3. Note that the Medians Method and Modified Mitchell's Method provide the best estimate with respect to the experimental result. Fig. 10(b) compares Principal Stress and Brown-Miller fatigue criteria on specimens without LSP using the Modified Mitchell's Method for Coffin-Manson parameters estimation; note that Principal Stress model provides a better estimate of fatigue life using Morrow and SWT equations to take into account the mean stress effect. Fig. 10(c) is similar to 10(b) but for LSP treated specimens.

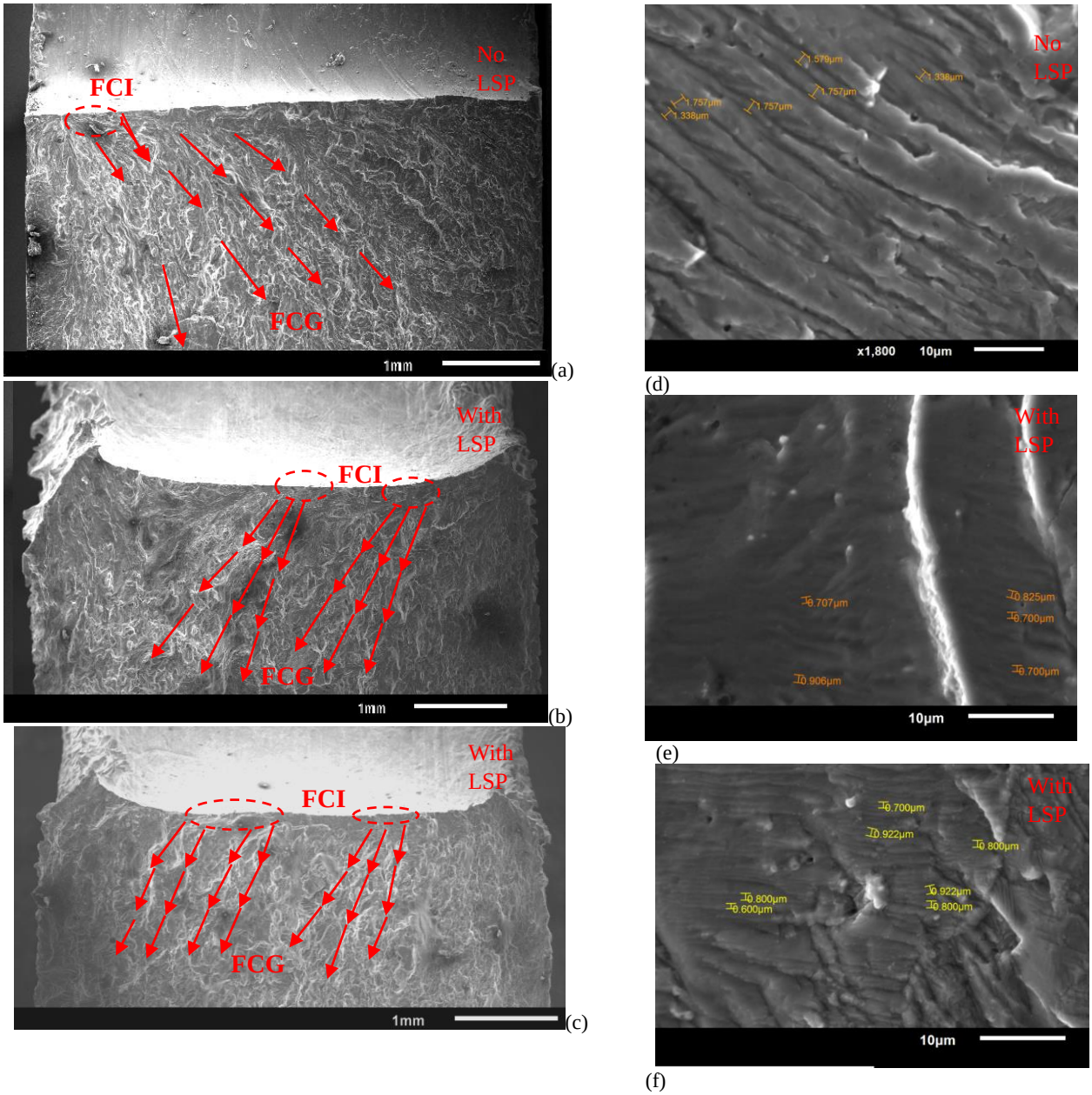

Fig. 12 (a)-(c) Fatigue crack initiation (FCI) and fatigue crack growth (FCG) directions; (d)-(f) striations due to stable fatigue crack growth. (a), (d) specimen without LSP, (b), (e) specimen with previous fatigue damage and then treated with LSP, (c), (f) specimen without previous damage treated with LSP

Note that again, the Principal Stress criterion for fatigue analysis provides a better life prediction using both, Morrow and SWT equations for mean stress effect. Note that results of Fig. 10 correspond to specimens without previous fatigue damage, that is, simulation for fatigue analysis considered LSP effect but only on damage-free specimens.

Fracture surface of a tested sample with LSP is shown in Fig. 11; the three main regions: crack initiation, crack growth and final rupture are amplified.

The effect of LSP on the location of fatigue crack initiation points is visualized in Fig. 12. Figs. 12(a) to 12(c) show SEM micrographs of the fatigue crack initiation (FCI) and growth (FCG) zones for different specimens. Specimen without LSP (Fig. 10(a)) shows FCI close to the specimen surface, while specimens with LSP (Figs. 10(b) and 10(c)) exhibit FCI points in the interior of the specimen; that is, LSP makes FCI point move from surface to the interior of the specimen, this fact is a consequence of the compressive residual stress field generated by LSP. This result is in agreement with a previous observation by Zhang *et al.* (2015). We demonstrate that on specimens with previous fatigue damage, the main location of fatigue crack initiation is also transferred from surface to sub-surface. Micrograph 12(c) corresponds to a specimen with LSP without previous fatigue damage and it shows that FCI occurs inside the specimen, this is in agreement with the predictions of the fatigue analysis shown in Fig. 9, where fatigue life

estimation exhibits a lower value at the middle of the treated specimen.

Figs. 12(d), (e) and (f) show the magnification views of 12(a), (b) and (c), respectively. Fatigue striations are found in all the fracture surfaces. Fig. 12(d) shows fatigue striations on the specimen without LSP where the striation spacing is in the range of 1.33-1.75 μm. Fig. 12(e) shows the fracture surface of the specimen with previous fatigue damage and then treated with LSP; the striation spacing was 0.7-0.9 μm. Fig. 12(f) shows the fracture surface of the sample treated with LSP without previous fatigue damage; the striation spacing was 0.6-0.9 μm. It is observed that LSP decreases striation spacing compared to untreated samples; this fact corresponds to a decrease in fatigue crack growth rate due to the LSP effect.

5. Conclusions

The influence of LSP on the fatigue crack initiation life of 6061-T6 aluminum samples with slots has been investigated. It was demonstrated that LSP extends the fatigue life of notched components with and without previous fatigue damage. It was observed that LSP extendeds fatigue crack initiation up to 58% on notched specimens with previous damage. Thus, LSP is a suitable technique to improve fatigue life of in-service damaged components with slots. LSP is a feasible technique not only to decrease fatigue crack growth rate, but also to decrease fatigue crack initiation.

LSP simulation by finite element method followed by a fatigue analysis provided good prediction of the onset of component failure. This simulation and analysis are powerful tools for process parameters definition and optimization as well as for component design, especially the design of components with geometric details such as notches.

Microscopic observations on the specimen fracture surfaces reveals details that are in agreement with simulation predictions. Compressive residual stresses generated by LSP make the fatigue crack initiation locations move from the surface to the sub-surface. Fatigue striation spacing on samples with LSP is lower than that of untreated specimens. A grain refinement is generated and the density of dislocations is increased, this fact is agreement with observations of Lu *et al*. (2010) and Zhou *et al.* (2012). An increase of sliding bands in the LSP treated specimens is observed as well, this phenomenon is not present in the middle of the specimens, where there is not LSP effect.

References

Achintha, M., Nowell, D., Fufari, D., Sackett, E.E. and Bache, M.R. (2014), "Fatigue behaviour of geometric features subjected to laser shock peening: Experiments and modelling", *Int. J. Fatigue*, **62**, 171-179.

Amrouche, A., Mesmacque, G., Garcia, S. and Talha, A. (2003), "Cold expansion effect on the initiation and the propagation of the fatigue crack", *Int. J. Fatigue*, **25**, 949-954.

ASTM (2013), Annual book of ASTM Standards, No. E837-13a Standard Test Method for Determining Residual Stresses by the Hole-Drilling Strain-Gauge Method.

Bäumel, A. Jr. and Seeger, T. (1990), Materials Data for Cyclic Loading, Supplement 1, Elsevier Science Publishers, Amsterdam.

Brown, M.W. and Miller, K.J. (1973), "A theory for fatigue failure under multiaxial stress–strain conditions", *Proc. Inst. Mech. Eng*., **187**(65), 745-755.

Chakherlou, T.N. and Vogwell, J. (2003), "The effect of cold expansion on improving the fatigue life of fastener holes", *Eng. Fail. Anal*., **10**(1), 13-24.

Correa, C., Ruiz de Lara, L., Díaz, M., Porro, J.A., García-Beltrán, A. and Ocaña, J.L. (2015), "Influence of pulse sequence and edge material effect on fatigue life of Al2024-T351 specimens treated by laser shock processing", *Int. J. Fatigue*, **70** , 196-204.

Cuellar, S.D., Hill, M.R., DeWald, A.T. and Rankin, J.E. (2012), "Residual stress and fatigue life in laser shock peened open hole samples", *Int. J. Fatigue*, **44**, 8-13.

Ding, K. (2003) "Three-dimensional dynamic finite element analysis of multiple laser shock peening processes", *Surface Eng.*, **19**(5), 351-358.

Ding, K. and Ye, L. (2006), "Simulation of multiple laser shock peening of a 35CD4 steel alloy", *J. Maters. Proc. Technol*., **178**(1), 162-169.

Dowling, N.E. (2007), Mechanical Behavior of Materials, Engineering Methods for Deformation, Fracture and Fatigue, Prentice-hall.

Fatigue theory reference manual (2002), FE-Safe documentation.

Goel, M.D. (2015), "A Numerical study of ogive shape projectile impact on multilayered", V. Matsagar, Advances in Structural Engineering mechanics, Springer, Nueva Delhi, 247-257.

Hatamleh, O. (2009), "A comprehensive investigation on the effects of laser and shot peening on fatigue crack growth in friction stir welded AA 2195 joints", *Int. J. Fatigue*, **31**, 974-988.

Hatamleh, O., Hill, M., Forth, S. and Garcia, D. (2009), "Fatigue crack growth performance of peened friction stir welded 2195 aluminum alloy joints at elevated and cryogenic temperatures", *Mater. Sci. Eng*. A, **519**(1), 61-69.

Hatamleh, O., Lyons, J. and Forman, R. (2007), "Laser and shot peening effects on fatigue crack growth in friction stir welded 7075-T7351 aluminum alloy joints", *Int. J. Fatigue*, **29**(3), 421-434.

Hfaiedh, N., Peyre, P., Song, H., Popa, I., Ji, V. and Vignal, V. (2015), "Finite element analysis of laser shock peening of 2050-T8 aluminum alloy", *Int. J. Fatigue*, **70**, 480-489.

Hong, Z. and Chengye, Y. (1998), "Laser shock processing of 2024-T62 aluminum alloy", *Mater. Sci. Eng. A*, **257**(2), 322-327.

Ivetic, G. (2011), "Three-dimensional FEM analysis of laser shock peening of aluminium alloy 2024-T351 thin sheets", *Surf. Eng*., **27**(6), 445-453.

Ivetic, G., Meneghin, I. and Troiani, E. (2011), "Numerical Analysis of Laser Shock Peening as a Process for Generation of Compressive Residual Stresses in Open Hole Specimens", *Mater. Sci. Forum*, **681**, 267-272.

Ivetic, G., Meneghin, I., Troiani, E., Molinari, G., Ocaña, J. L., Morales, M., Porro, J., Lanciotti, A., Ristori, V., Polese, C., Plaisier, J. and Lausi, A. (2012), "Fatigue in laser shock peened open-hole thin aluminium specimens", *Mater. Sci. Eng. A*, **534**, 573-579.

Kandil, F.A., Brown, M.W. and Miller, K.J. (1982), "Biaxial low-cycle fatigue fracture of 316 stainless steel at elevated temperatures", *The Metals Society*, **280**, London.

Lacarac, V., Smith, D.J., Pavier, M.J. and Priest, M. (2000), "Fatigue crack growth from plain and cold expanded holes in aluminium alloys", *Int. J. Fatigue*, **22**(3), 189-203.

Lavender, C.A., Honga, S.T., Smith, M.T., Johnson, R.T. and Lahrman, D. (2008), "The effect of laser shock peening on the life and failure mode of a cold pilger die", *J. Maters. Proc. Technol*., **204**(1), 486-491.

Li, J., Zhang, Z., Sun, Q., Li, C. and Li, R. (2011), "A modified method to estimate fatigue parameters of wrought aluminum alloys", *J. Mater. Eng. Perform*., **20**(7), 1323-1329.

Liu, J., Shao, X.J., Liu, Y.S. and Yue, Z.F. (2008), "Effect of cold expansion on fatigue performance of open holes", *Mater. Sci. Eng. A*, **477**(1), 271-276.

Lu J.Z., Luoc, K.Y., Zhang, Y.K., Sun, G.F., Gu, Y.Y., Zhou, J.Z. and Ren, X.D. (2010), "Grain re- finement mechanism of multiple laser shock processing impacts on ANSI 304 stainless steel", *Acta Metall*, **58**(16), 5354-5362.

Meggiolaro, M.A. and Castro, J.T.P. (2004), "Statistical evaluation of strain-life fatigue crack initiation predictions", *Int. J. Fatigue*, **26**(5), 463-476.

Ocaña, J.L., Morales, M., Molpeceres, C. and Torres, J. (2004) "Numerical simulation of surface deformation and residual stresses fields in laser shock processing experiments", *Appl. Surface Sci.*, **238**(1), 242-248.

Park, J.H. and Song, J.H. (2003), "New estimation method of fatigue properties of aluminum alloys", *J. Eng. Mater. Technol*., **125**(2), 208-214.

Peyre, P. and Fabbro, R. (1995), "Laser shock processing: a review of the physics and applications", *Opt. Quant. Electron*. **27**(12), 1213-1229.

Ren, X.D., Zhan, Q.B., Yang, H.M., Dai, F.Z., Cui, C.Y., Sun, G.F. and Ruan, L. (2013), "The effects of residual stress on fatigue behavior and crack propagation from laser shock processing-worked hole", *Mater. Des*., **44**, 149-154.

Rubio-González, C., Felix-Martinez, C., Gomez-Rosas, G., Ocaña, J.L., Morales, M. and Porro, J. (2011), "Effect of laser shock processing on fatigue crack growth of duplex stainless steel", *Mater. Sci. Eng. A*, **528**(3), 914-919.

Rubio-González, C., Gomez-Rosas, G., Ocaña, J.L., Molpeceres, C., Banderas, A., Porro, J. and Morales M. (2006), "Effect of an absorbent overlay on the residual stress field induced by laser shock processing on aluminum samples", *Appl. Surf. Sci*., **252**(18), 6201-6205.

Rubio-Gonzalez, C., Gomez-Rosas, G., Ruiz, R., Nait, M. and Amrouche, A. (2015), "Effect of laser shock peening and cold expansion on fatigue performance of open hole samples", *Struct. Eng. Mech*., **53**(5), 867-880.

Rubio-González, C., Ocaña, J.L., Gomez-Rosas, G., Molpeceres, C., Paredes, M., Banderas, A., Porro, J. and Morales, M. (2004), "Effect of laser shock processing on fatigue crack growth and fracture toughness of 6061-T6 aluminum alloy", *Mater. Sci. Eng. A*, **386**(1), 291-295.

Sánchez-Santana, U., Rubio-Gonzalez, C., Gomez-Rosas, G., Ocaña, J.L., Molpeceres, C., Porro, J. and Morales, M. (2006), "Wear and friction of 6061-T6 aluminum alloy treated by laser shock processing", *Wear*, **260**(7), 847-854.

Tsay, L.W., Young, M.C. and Chen, C. (2003), "Fatigue crack growth behavior of laser-processed 304 stainless steel in air and gaseous hydrogen", *Corr. Sci*., **45**(9), 1985-1997.

Yang, J.M., Her, Y.C., Han, N. and Clauer A. (2001), "Laser shock peening on fatigue behavior of 2024-T3 Al alloy with fastener holes and stopholes", *Mater. Sci. Eng. A*, **298**(1), 296-299.

Zhang, X.Q., Li, H., Yu, X.L., Zhou, Y., Duan, S.W., Li, S.Z., Huang, Z.L. and Zuo, L.S. (2015), "Investigation on effect of laser shock processing on fatigue crack initiation and its growth in aluminum alloy plate", *Mater. Des*., **65**, 425-431.

Zhou, J.Z., Huang, S., Sheng J., Lu, J.Z., Wang, C.D., Chen, K.M., Ruan, H.Y. and Chen, H.S. (2012), "Effect of repeated impacts on mechanical properties and fatigue fracture morphologies of 6061-T6 aluminum subject to laser peening", *Mater. Sci. Eng. A*, **539**, 360-368.

PL